Coherent vibrational dynamics of intermolecular hydrogen bonds in acetic acid dimers studied by ultrafast mid-infrared spectroscopy

2003 J. Phys.: Condens. Matter 15 S129

(http://iopscience.iop.org/0953-8984/15/1/316)

INSTITUTE OF PHYSICS PUBLISHING JOURNAL OF PHYSICS: CONDENSED MATTER

J. Phys.: Condens. Matter **15** (2003) S129–S136 PII: S0953-8984(03)55205-5

Coherent vibrational dynamics of intermolecular hydrogen bonds in acetic acid dimers studied by ultrafast mid-infrared spectroscopy

Karsten Heyne, Nils Huse, Erik T J Nibbering and Thomas Elsaesser

Max-Born-Institut für Nichtlineare Optik und Kurzzeitspektroskopie, D-12489 Berlin, Germany

Received 24 October 2002
Published 16 December 2002
Online at stacks.iop.org/JPhysCM/15/S129

Abstract

Ultrafast vibrational motions and the underlying microscopic couplings in hydrogen-bonded cyclic dimers of acetic acid are studied by pump–probe and photon echo experiments in the mid-infrared. Upon femtosecond excitation of the O–H stretching mode, we demonstrate coherent nuclear motions along the in-plane dimer stretching mode which persist for picoseconds. The anharmonic coupling of the O–H stretching and the low-frequency mode is isolated in the nonlinear vibrational response, whereas other couplings are suppressed. Three-pulse photon echo experiments demonstrate a dephasing of O–H stretching excitations on a femtosecond timescale and quantum beats due to the anharmonically coupled dimer stretching mode.

1. Introduction

Single and multiple hydrogen bonds stabilize important structural motifs in Nature such as the double-helix DNA structure [1], the α-helix and β-sheet protein conformations [2], and the structure of hydrogen-bonded liquids such as water [3]. Hydrogen bonds are—on the other hand—weak enough to allow structural changes on a multitude of timescales, e.g., in hydrogen transfer processes or protein folding. Both the static and dynamic aspects of hydrogen bonds have been investigated using a variety of experimental techniques and theoretical concepts [4]. In particular, vibrational spectroscopy gives insight into local properties of hydrogen-bonded groups and—thus—the geometry and strength of hydrogen bonds.

Steady-state linear infrared spectroscopy has concentrated on stretching bands of hydrogen donor groups, e.g., O–H, revealing a pronounced red-shift of the stretching frequency, very strong spectral broadening, and peculiar spectral substructure as indicative for the formation of a hydrogen bond. Although sophisticated theoretical models have been developed for describing this behaviour, the spectral envelopes of most stretching bands are not understood in detail. This lack of specific knowledge is mainly due to the occurrence of different microscopic mechanisms of similar strength leading to rather congested vibrational lineshapes [4–7]. In addition to intramolecular couplings, the interaction with the liquid environment plays an

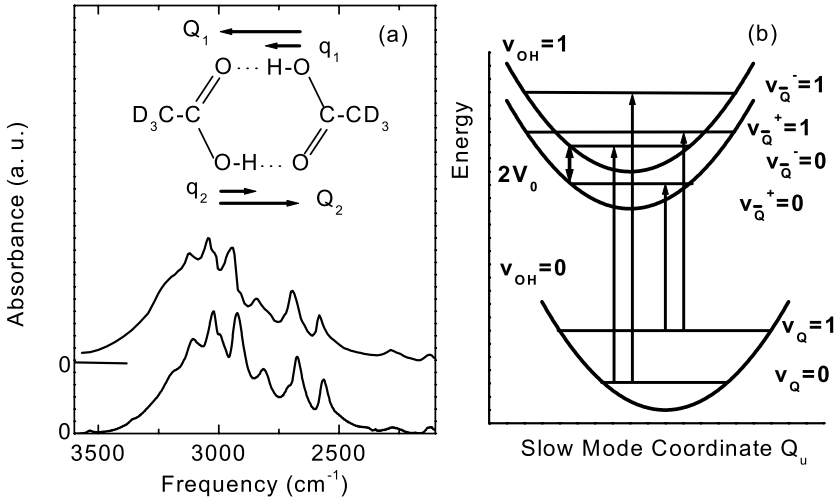

Figure 1. (a) Top: a schematic diagram of the cyclic acetic acid dimer including the high-frequency ($q_{1,2}$) and low-frequency ($Q_{1,2}$) local mode coordinates. Bottom: steady-state O–H stretching absorption of cyclic acetic acid dimers in the gas phase (upper spectrum) and in liquid CCl_4 (lower spectrum). (b) Potential energy surfaces in the $v_{O-H} = 0$ and 1 states including the two lowest vibrational levels of the low-frequency mode as a function of the symmetrized low-frequency mode Q_u. The Davydov splitting V_0 leads to two different series of vibrational transition lines from the $v_{O-H} = 0$ to 1 state split by $2V_0$.

important role. Time-resolved nonlinear vibrational spectroscopy has the potential to separate the different coupling processes via their different microscopic dynamics occurring in the ultrafast time domain between approximately 10 fs and 10 ps. Such techniques have provided substantial information on a variety of hydrogen-bonded systems [8–11]. In this paper, we present new results on an important model system for coupled intermolecular hydrogen bonds, the cyclic acetic acid dimer. Femtosecond three-pulse photon echo and pump–probe experiments demonstrate pure dephasing processes on a femtosecond timescale, leading to homogeneous broadening, as well as anharmonic coupling of the O–H stretching mode to intermolecular low-frequency modes.

2. Lineshape of the hydrogen-bonded O–H stretching band

The O–H stretching band of the cyclic dimer of acetic acid in the gas and the liquid phase has been investigated in great detail [4–6]. In figure 1, the gas phase spectrum and the spectrum of dimers dissolved in CCl_4 are shown, together with the molecular geometry. Upon hydrogen bonding, the O–H stretching band displays a strong red-shift due to a reduced force constant, a broadening, and a pronounced substructure. These spectral features have been ascribed to the following mechanisms (see [5–7], figure 1(b)):

(i) Anharmonic coupling: anharmonic coupling of low-frequency modes to the high-frequency stretching motion leads to the formation of vibrational sidebands and—thus—to a broadening of the overall band. As the timescales of the low-and high-frequency motions are distinctly different, this mechanism has been described in a Born–Oppenheimer-like picture, resulting in quantized levels of the low-frequency mode on potential energy surfaces determined by the high-frequency mode, and in Franck–Condon progressions

of vibrational lines. Direct experimental evidence for this mechanism has recently been found in single intramolecular hydrogen bonds [10] but so far not for hydrogen-bonded dimers.

(ii) Davydov or excitonic coupling: in general, there exists a coupling V_0 between the two O–H stretch oscillators in the dimers. Taking into account both anharmonic and Davydov coupling, a complex lineshape results. This is visualized with the help of figure 1(b) showing the vibrational energy as a function of the coordinate $Q_u = (Q_1 - Q_2)/2^{1/2}$ where $Q_{1,2}$ are the local low-frequency coordinates of the two hydrogen bonds. The excitonic coupling V_0 leads to two potential minima in the $v_{\mathrm{O-H}} = 1$ state which are shifted by $2V_0$. There are two separate progressions originating from the $v_Q = 0$ and 1 levels in the $v_{\mathrm{O-H}} = 0$ state. On the basis of this model, the gas phase O–H stretching band of acetic acid dimers has been reproduced quantitatively, assuming a frequency of 110 cm^{-1} for the low-frequency mode, an anharmonic coupling $\alpha = 1.5$, and a Davydov splitting of $V_0 = -90$ cm^{-1} [5]. Later work [6], however, suggests much smaller V_0-values and other sets of parameter values reproducing the spectra equally well. Thus, there is no unambiguous information to be extracted from the steady-state spectra.

(iii) Fermi resonances between the O–H stretching mode and overtones or combination bands may introduce additional splittings within the O–H stretching band, leading to characteristic dips of absorption denoted as Evans windows [7].

(iv) Homogeneous and inhomogeneous line broadening: overdamped intramolecular or solvent modes exert a fluctuating force on the O–H stretching vibration that, depending on the modulation strength and timescale, may vary between a distribution of transition frequencies (inhomogeneous broadening) or a single motionally narrowed transition (homogeneous broadening).

In the following, we present results from ultrafast pump–probe and photon echo experiments, allowing a separation of different contributions to the overall lineshape.

3. Experiment

In the pump–probe experiment, we studied a solution of 0.8 M acetic acid (CD_3COOH, 99% deuteration grade) in CCl_4 which is held between two CaF_2 windows with a 100 μm thick spacer. This sample is excited by an intense mid-infrared pump pulse, promoting dimers $(CD_3COOH)_2$ from the $v_{\mathrm{O-H}} = 0$ to 1 state in which one of the O–H stretching oscillators is excited. The resulting change of vibrational absorption is monitored by a weak probe pulse as a function of the pump–probe delay. The probe pulse is spectrally dispersed after interaction with the sample and detected with a 2×16-element HgCdTe array (spectral resolution 4–9 cm^{-1}). Femtosecond mid-infrared pulses tunable throughout the O–H stretching band were generated by parametric frequency conversion of regeneratively amplified pulses from a mode-locked Ti:sapphire laser with a repetition rate of 1 kHz [12]. The pulse duration was 110 fs, the spectral pulse width approximately 140 cm^{-1} (FWHM).

Three-pulse photon echo experiments were performed in the so-called box configuration: thee overlapping beams with wavevectors $\boldsymbol{k}_1$, $\boldsymbol{k}_2$, and $\boldsymbol{k}_3$ were focused onto the sample and nonlinear signals diffracted from the transient grating in the sample were detected in the directions $\boldsymbol{k}_3 + \boldsymbol{k}_2 - \boldsymbol{k}_1$ and $\boldsymbol{k}_3 - \boldsymbol{k}_2 + \boldsymbol{k}_1$. The photon echo signals were measured as a function of the coherence time τ, the delay between the two pulses generating the transient grating in the sample, and as a function of the population time T, the delay between the second and the third pulse which is diffracted from the sample. Three mid-infrared pulses of up to 3 μJ energy, 100 fs duration, and parallel polarization were used in the experiments. A 0.2 M solution of

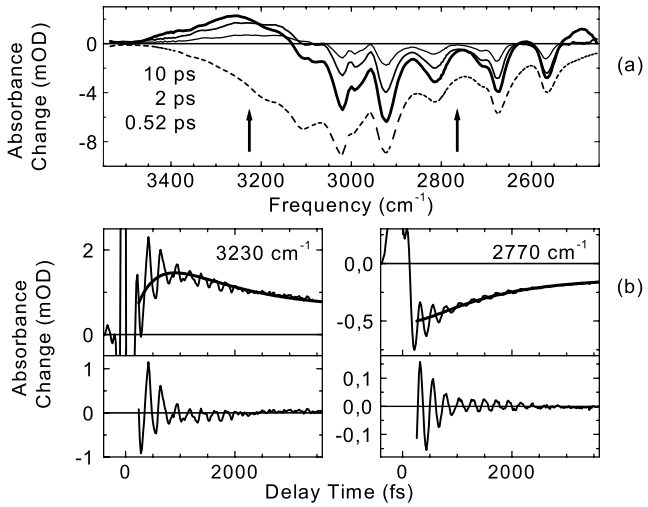

Figure 2. (a) Transient difference absorption spectra for time delays of 0.52, 2, and 10 ps between pump and probe pulses. The change of absorbance $\Delta A = -\log_{10}(T/T_0)$ is plotted versus probe frequency (T, T_0: sample transmission with and without excitation). The arrows indicate the probe position of the transients shown in (b). Dashed curve: inverted absorption spectrum. (b) Upper panels: absorbance change as a function of pump–probe delay at fixed probe frequencies. Numerical fits of the incoherent dynamics are shown as smooth curves. The oscillatory part of the transients is plotted in the lower panels.

acetic acid in CCl_4 was pumped through a 200 μm thick flow cell in order to suppress thermal accumulation effects induced by the intense infrared pulses. The photon echo signals were detected with a cooled InSb detector (homodyne detection).

4. Results and discussion

Results of the pump–probe experiments are presented in figure 2. In figure 2(a), the change of absorbance ΔA is plotted as a function of probe frequency for different delay times. The spectrum taken at a delay time of 0.52 ps shows a predominant decrease of absorption (bleaching, negative sign) between 2600 and 3100 cm^{-1} and an enhanced absorption (positive sign) on the low- and high-energy tails of the steady-state band (dashed curve). The enhanced absorption at low frequencies decays within the first 2 ps whereas the absorption increase at high frequencies persists substantially longer.

In figure 2(b), time-resolved signals are plotted for the two spectral positions indicated in figure 2(a). For a temporal overlap of pump and probe pulses, i.e. around delay zero, one finds a strong signal caused by the third-order nonlinearity of the solvent and/or windows of the sample cell, exceeding the ordinate scale of figure 2(b). For positive delay times, i.e. sequential interaction of pump and probe with the sample, a rate-like increase or decrease of absorption is observed which is superimposed by strong oscillations (upper panels in figure 2(b)). To extract the pronounced oscillatory signals, the incoherent absorption changes were fitted by a rate equation model (smooth curves in the upper panels of figure 2(b)) which will be discussed in detail elsewhere, and subtracted from the total signal. The resulting oscillatory components in the lower panels of figure 2(b) exhibit an oscillation period of 220 fs, a damping on a timescale of 2–3 ps and—at 2770 cm^{-1}—clear signatures of a beating pattern on the oscillation

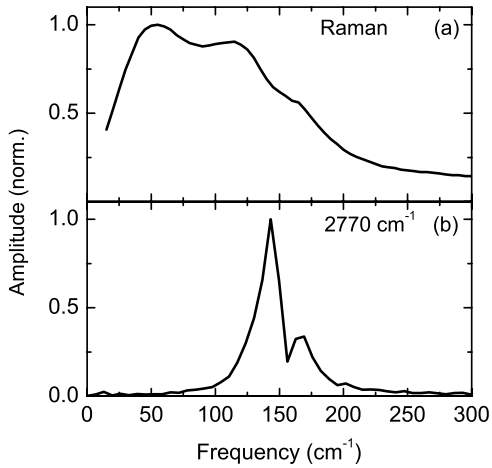

Figure 3. (a) The steady-state low-frequency Raman spectrum of CH_3COOH (13). (b) The Fourier spectrum of the oscillatory signal measured at 2770 cm^{-1}, displaying two components at 145 and 170 cm^{-1}.

amplitudes. This is also evident from the Fourier transform of this oscillatory transient in figure 3(b), displaying two prominent contributions at 145 and 170 cm^{-1}.

The decrease of absorption in the transient spectra (figure 2(a)) is due to the pump-induced depletion of the $v_{O-H} = 0$ ground state and to stimulated emission from the transient excess population of the $v_{O-H} = 1$ state. The latter also underlies the enhanced absorption at frequencies below 2550 cm^{-1} which is caused by the $v_{O-H} = 1 \rightarrow 2$ transition. The $v_{O-H} = 1$ population decays within the first 2 ps, transferring the excess energy provided by the pump photon into other vibrations. After this process, the dimer with a heated vibrational manifold populates the ground state. The heating results in a weakening of the intermolecular hydrogen bonds—an effect that has been observed also in other hydrogen-bonded systems [10]—and a concomitant blue-shift of the O–H stretching absorption, underlying the enhanced absorption above 3100 cm^{-1}. The hot ground state of the dimer cools down to its initial temperature by an intermolecular transfer of excess energy to the solvent within tens of picoseconds, leading the slow decay of both transients in figure 2(b).

Superimposed on such incoherent signals are pronounced oscillations (figure 2(b)) which display frequency components of 145 and 170 cm^{-1} (figure 3(b)) throughout the O–H stretching band. Such coherent signals are due to the generation of vibrational wavepackets in the $v_{O-H} = 0$ and $v_{O-H} = 1$ states by the broadband pump pulse: within the spectral (electric field) envelope of the pump, several lines of the progressions in the low-frequency mode (cf figure 1(b)) are driven coherently, creating a superposition of several levels of the low-frequency mode in the $v_{O-H} = 1$ state. A similar wavepacket is generated in the $v_{O-H} = 0$ state through an impulsive resonantly enhanced Raman process within the pump bandwidth. The coherent motion of the wavepackets modulates the length of the two hydrogen bonds in the dimer and—thus—the O–H stretching absorption as shown in figure 2(b). The wavepacket motion is damped by vibrational dephasing on a comparably slow timescale of several picoseconds, clearly demonstrating the underdamped character of the low-frequency mode.

It is interesting to compare the Fourier spectrum of the oscillations with the low-frequency Raman spectrum of acetic acid (see [13], figure 3(a)). We attribute the oscillations to the 165 cm^{-1} Raman mode which is connected with an in-plane dimer stretching motion. The

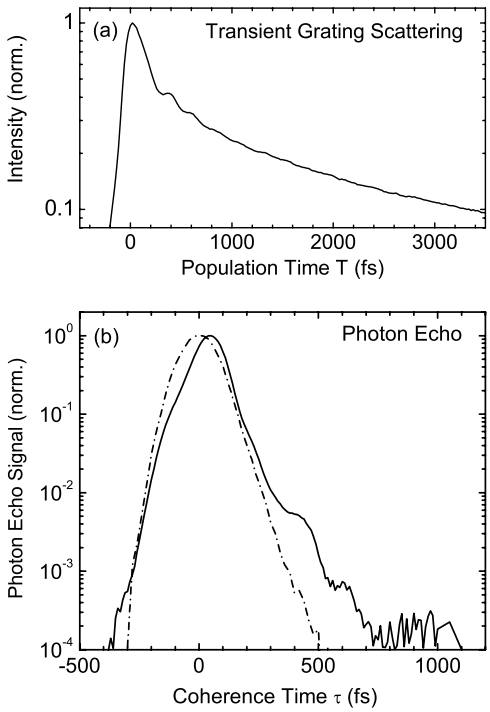

Figure 4. (a) The transient grating signal from the acetic acid solution. The intensity diffracted from the sample is plotted on a logarithmic scale as a function of the population time T. (b) Normalized two-pulse photon echo signals from the acetic acid solution (solid curve) and the pure solvent CCl_4 (dash–dotted curve) measured at a frequency of 2830 cm^{-1}. The diffracted intensity is plotted as a function of the coherence time τ (population time $T = 0$).

double-peak structure in the Fourier spectrum of figure 3(b) points to different frequencies and phases of the coherent wavepacket motion in the $v_{O-H} = 0$ and 1 states. Upon excitation to the $v_{O-H} = 1$ state, the hydrogen bonds become shorter, i.e. stronger (negative origin shift in figure 1(b)), suggesting a frequency upshift from 145 cm^{-1} in the $v_{O-H} = 0$ to 170 cm^{-1} in the $v_{O-H} = 1$ state.

Oscillatory signals due to the Davydov splitting V_0 (figure 1(b)) are completely absent in the pump–probe signals. The two Davydov-shifted progressions originate from different molecules in which either the $v_Q = 0$ or 1 level in the $v_{O-H} = 0$ state is populated. The pump–probe signal is proportional to the sum of polarization components from these two subsets of molecules, i.e. there is no polarization interference that could give rise to beats with a frequency corresponding to $2V_0$. This observation underlines the inherent strength of nonlinear spectroscopy in separating different microscopic couplings.

We now present the first three-pulse photon echo results for O–H stretching excitations of carboxylic acid dimers. In a transient grating scattering experiment at 2830 cm^{-1}, i.e. close to the centre of the O–H stretching band, the first two pulses with zero mutual delay (coherence time $\tau = 0$) generate a population grating from which the third pulse delayed by the population time T is scattered. This signal (figure 4(a)) measured as a function of T exhibits the incoherent population kinetics of the O–H stretching oscillator and is superimposed by coherent oscillations due to the anharmonically coupled low-frequency mode. Both the incoherent decay kinetics and the oscillation period of 220 fs are in very good agreement with the pump–

probe data. In figure 4(b), photon echo data taken at the same spectral position are shown. The intensity diffracted into the direction $\boldsymbol{k}_3 + \boldsymbol{k}_2 - \boldsymbol{k}_1$ is plotted on a logarithmic scale as a function of the coherence time τ, the delay between the two pulses generating the transient grating (solid line). The measurements were performed with a population time $T = 0$, corresponding to a two-pulse photon echo. One finds a very fast decay of the coherent O–H stretching polarization resulting in a decrease of the photon echo signal by four orders of magnitude within 700 fs, much faster than the population decay in figure 4(a). Thus, the decay of the macroscopic O–H stretching polarization is dominated by pure dephasing processes whereas the population decay makes a minor contribution. Similarly fast photon echo decays have been observed with other hydrogen-bonded systems such as water and phthalic acid monomethyl ester [11, 14]. The photon echo signal in figure 4(b) displays weak oscillatory features which are evident from the slight modulation of the decay and the shoulder around $\tau = 450$ fs. Within the experimental accuracy, the period of the oscillatory signal is identical to that in the pump–probe and transient grating data and points to a quantum beat caused by the wavepacket motion along the anharmonically coupled low-frequency mode.

The broadband femtosecond pulses generate coherent polarizations on a multitude of lines of the vibrational progressions within the O–H stretching band. Thus, the photon echo decay is a complex superposition of the polarization decays on such individual transitions which are modulated by the low-frequency wavepackets. Under such conditions, extraction of a dephasing time from the overall photon echo decay requires a detailed theoretical modelling which is beyond the scope of this paper. A lower limit of the dephasing time of individual transitions can, however, be estimated from the pump–probe data in figure 2(a) displaying pronounced spectral holes. The spectral position of such holes remains the same for tens of picoseconds, i.e. spectral diffusion within the band plays a minor role. In this case and for the very weak saturation of the absorption in our experiments, the width of the spectral holes is determined by the homogeneous linewidth of the underlying transition. The spectral holes in figure 2(a) show a width of about 50 cm^{-1} corresponding to a dephasing time $T_2 \geqslant 200$ fs.

In conclusion, our results give important new information on the microscopic couplings between vibrational excitations in hydrogen-bonded dimers. Anharmonic coupling of the fast O–H stretching motion to intermolecular low-frequency motions of the cyclic acetic acid dimer allows the generation of coherent wavepacket motions along a low-frequency mode which modulates the length of the hydrogen bonds. This low-frequency dimer stretching mode is underdamped and—thus—wavepacket motion persists for several picoseconds. This may in future allow for optically controlling nuclear motions and inducing elementary chemical reactions such as hydrogen transfer by repetitive interaction with phase-shaped ultrashort pulses. The photon echo experiments show a fast homogeneous dephasing of the O–H stretching mode superimposed by quantum beats due to the coherent low-frequency motions.

Acknowledgment

This work was supported by the Deutsche Forschungsgemeinschaft through the Sonderforschungsbereich 450 ‘Analysis and control of ultrafast photoinduced reactions’.

References

[1] Watson J D and Crick F H C 1953 *Nature* **171** 737
[2] Creighton T E 1992 *Proteins: Structures and Molecular Properties* (New York: Freeman)
[3] Franks F (ed) 1972–1981 *Water: a Comprehensive Treatise* (New York: Plenum)
[4] Schuster P, Zundel G and Sandorfy C (ed) 1976 *The Hydrogen Bond* (Amsterdam: North-Holland)

[5] Maréchal Y and Witkowski A 1968 *J. Chem. Phys.* **48** 3697
[6] Maréchal Y 1987 *J. Phys. Chem.* **87** 6344
[7] Chamma D and Henri-Rousseau O 1999 *Chem. Phys.* **248** 53
Chamma D and Henri-Rousseau O 1999 *Chem. Phys.* **248** 71
[8] Woutersen S W, Emmerichs U and Bakker H 1997 *Science* **278** 658
[9] Gale G M, Gallot G, Hache G, Lascoux N, Bratos S and Leicknam J C 1999 *Phys. Rev. Lett.* **82** 1086
[10] Stenger J, Madsen D, Dreyer J, Nibbering E T J, Hamm P and Elsaesser T 2001 *J. Phys. Chem.* A **105** 2929
[11] Stenger J, Madsen D, Hamm P, Nibbering E T J and Elsaesser T 2001 *Phys. Rev. Lett.* **87** 027401
[12] Kaindl R A, Wurm M, Reimann K, Hamm P, Weiner A M and Woerner M 2000 *J. Opt. Soc. Am.* B **17** 2086
[13] Nakabayashi T, Kosugi K and Nishi N 1999 *J. Phys. Chem.* A **103** 8595
[14] Stenger J, Madsen D, Dreyer J, Hamm P, Nibbering E T J and Elsaesser T 2002 *Chem. Phys. Lett.* **354** 256